scientific reports

Check for updates

OPEN

A primate model animal revealed the inter-species differences and similarities in the subtype specifications of the spiral ganglion neurons

Makoto Hosoya✉, Masafumi Ueno, Marie N. Shimanuki, Takanori Nishiyama, Naoki Oishi & Hiroyuki Ozawa

Type I spiral ganglion neurons are peripheral neurons essential for hearing perception. While they can be subdivided in mice based on characteristic gene expression patterns, detailed examinations of these subtypes in primates and humans are lacking. In this study, we investigated the developmental subtypes of spiral ganglion neurons in the common marmoset (*Callithrix jacchus*). We confirmed that Type I spiral ganglion can be divided based on the characteristic gene expression patterns of several marker genes. However, some combinations of these genes differ from those in rodents, suggesting common marmoset's suitability for advancing our understanding of human cochlear development. Additionally, identifying the essential time points for subtype specifications and subsequent maturation will aid in studying the primate-specific developmental biology of the inner ear. This could lead to new treatment strategies for hearing loss in humans and be valuable for studying age-related hearing loss, as well as designing regenerative therapies.

Keywords Cochlea, Marmoset, Rodents, Spiral ganglion neuron, Cochlear development

Spiral ganglion neurons are essential peripheral neurons involved in hearing perception. Spiral ganglion neurons can be divided into Types I and II[1,2]. Type I spiral ganglion neurons form synapses between the inner hair cells, in which sound waves are converted into electrical neuro-activity. These electrical pulses are conducted to the brain through Type I spiral ganglion neurons, which leads to hearing perception. Type II spiral ganglion neurons form synapses between the outer hair cells and modulate hearing activity. Previous studies have revealed that Type I spiral ganglion neurons can be subdivided into three subtypes in rodents based on both electrophysiological characteristics and gene expression patterns[3–6]. In recent studies, differences in the characteristics of each subtype have been employed to explain the wider dynamic ranges of our hearing perception and the clinical changes in hearing abilities as we age[7,8]. However, this subtype specification in cochlear development is not fully understood in humans or primates.

Previous electrophysiological examinations have revealed that Type I spiral ganglion neurons can be categorized based on intensity-dependent activation and sensitivity to sound[9–14]. High spontaneous firing rate neurons accompanying low sound threshold ("High-SR" neurons) tend to innervate the pillar side of the inner hair cells. Conversely, low spontaneous firing rate neurons with a high sound threshold ("Low-SR" neurons) tend to innervate the modiolar side of the inner hair cells. Additionally, "Mid-SR" neurons, characterized by an intermediate spontaneous firing rate and sound threshold, innervate between the high-SR neurons and low-SR neurons to inner hair cells[3].

Type I spiral ganglion neurons can also be divided according to gene expression patterns using single-cell RNASeq in the mouse cochlea[4–6]: type Ia, Ib, and Ic neurons. Previous studies based on gene expression patterns have shown that these subtypes are characterized by several marker genes: *Calb2* for Ia and Ib (high expression in Ia and moderate expression in Ib), *Calb1* and *Ttn* for Ib, *Pou4f1* and *Lypd1* for Ic, and *Runx1* for Ib and Ic[4,5,15,16]. Definitive proof of the identity of these subtypes, whether divided depending on electrophysiological activities

Department of Otorhinolaryngology, Head and Neck Surgery, Keio University School of Medicine, 35 Shinanomachi, Shinjuku-ku, Tokyo 160-8582, Japan. ✉email: mhosoya1985@keio.jp

or gene expression patterns, is not yet available. However, correlative data suggest that these three subtypes correspond to "High-SR neurons" in Type Ia, "Low-SR neurons in Type Ic, and "Mid-SR neurons" in Type Ib[8,17].

Recently, the developmental process of the specification of this subtype of spiral ganglion neurons has been investigated using rodent models. Previous studies have shown that the subtype specification started by dividing two larger branches: the type Ia, II branch, and the type Ib, Ic branch[5]. After that, these branches are differentiated into subtypes. Several transcription factors and related genes, such as *Pou4f1*, *Lypd1*, and *Runx1*, have been reported to determine subtype specifications. The developmental process of this subtype specification of spiral ganglion neurons has only been examined in rodent models because of the limited sampling of human fetuses and ethical concerns. However, recent studies have reported inter-species differences in cochlear development between rodents and primates[18,19]. In addition, knowledge about cochlear development derived from rodent models could not always be applicable to primate[19,20]. For example, the expression of *Calb1*, which is used as a type Ib marker in mice[4,21], is different from mice to a primate; its expression could be observed only in Type II neurons and not be detected in Type I spiral ganglion neurons in the postnatal cochlea of a primate model animal[22].

Our previous study revealed that the common marmoset, a non-human primate model animal, is a suitable alternative for human cochlear development[19]. In the present study, we examined the developmental subtype-specification of spiral ganglion neurons to clarify the extent of inter-species differences observed in a rodent model and the common marmoset. Our aim was to estimate the transferability of knowledge regarding spiral ganglion neurons subtypes obtained from rodents to primates. To our knowledge, this is the first report addressing the identification of subtypes of the Type I spiral ganglion neurons in cochlear development in primates.

Materials and methods

Cadaveric temporal bone samples from common marmoset fetuses at E77 (n = 2), E87 (n = 3), E92 (n = 3), E97 (n = 3), E101 (n = 2), E109 (n = 3), E120 (n = 3), P0 (n = 3) were used in this study, as described in our previous reports[19,23,24]. Adult animals were anesthetized via isoflurane inhalation (1.5–4%). Caesarion section was performed as previously described[25]. Animal experiments were approved by the Animal Experiment Committee of Keio University (approval numbers: 11006, 08,020) and performed in accordance with ARRIVE guidelines and the guidelines of the National Institutes of Health and the Ministry of Education, Culture, Sports, Science, and Technology of Japan.

Embryos were anesthetized on ice deeply and dissected in phosphate-buffered saline (PBS). The temporal bones were dissected immediately after euthanasia and fixed overnight in 4% paraformaldehyde in PBS. The specimens were embedded in Tissue-Tek O.C.T. compound (Sakura Fine Technical Co., Ltd., Tokyo, Japan) for cross-sectioning. P0 specimens were decalcified in Decalcifying Solution B (Wako, Osaka, Japan) for one week and embedded in Tissue-Tek O.C.T. compound (Sakura Finetechnical Co., Ltd., Tokyo, Japan) for cross-sectioning, as described in our previous reports. For immunohistochemical analysis, we used seven-micrometer sections.

The following primary antibodies were used: Anti-CALB2 (ms IgG1, BD610908, BD, Franklin Lakes, NJ, USA, 1:500; rb IgG, GTX103261, GeneTex, Irvine, CA, USA, 1:500), Anti-TUBB3 (ms IgG2a, 801,201, BioLegend, 1:500; ms IgG2b, T8660, Merck, 1:500), Anti-MYO7A (Rabbit IgG, 25–6790, Proteus Biosciences, Ramona, CA, USA, 1:500), Anti-PRPH (Chick IgY, ab39374, Abcam, Cambridge, UK, 1:500), Anti-NEFH (Chick IgY, ab4680, Abcam, Cambridge, UK, 1:1000), Anti-RBFOX3 (ms IgG1, MAB377, Merck Millipore, Burlington, MA, USA, 1:200), Anti-ISL1 (rb IgG, ab109517, Abcam, Cambridge, UK, 1:300), Anti-SOX10 (Mouse IgG1, 365,692, Santa Cruz Biotechnology, Santa Cruz, CA, USA, 1:200), Anti-POU4F1 (ms IgG2b, sc-8429, Santa Cruz Biotechnology, Santa Cruz, CA, USA, 1:200), Anti-ATOH1 (rb IgG, 21,215–1, Proteintech, Rosemont, IL, USA, 1:500) Anti-AML1 (rb IgG, #4336 (D33G6), Cell Signaling, 1:200), Anti-POU4F3 (ms IgG1, sc81980, Santa Cruz Biotechnology, Santa Cruz, CA, USA, 1:200), Anti-TLE4 (ms IgG1, sc365406, Santa Cruz Biotechnology, Santa Cruz, CA, USA, 1:100), Anti-GATA3 (ms IgG1, sc268, Santa Cruz Biotechnology, Santa Cruz, CA, USA, 1:50), Anti-ID1 (ms IgG2a, sc133104, Santa Cruz Biotechnology, Santa Cruz, CA, USA, 1:50), Anti-TTN (ms IgM, 9D-10-C, DSHB, Iowa City, IA, USA, 1:100), Anti-NCALD (rb IgG, 12,925–1, Proteintech, Rosemont, IL, USA, 1:300), Anti-TRIM54 (rb IgG, 21,074–1, Proteintech, Rosemont, IL, USA, 1:500), and Anti-INA (rb IgG, GTX133356, GeneTex, Irvine, CA, USA, 1:1000).

The following secondary antibodies were used: goat anti-rabbit IgG, Alexa Fluor Plus 555 (A32732, Invitrogen, Waltham, MA, USA, 1:500), goat anti-rabbit IgG, Alexa Fluor Plus 647 (A32733, Invitrogen, Waltham, MA, USA, 1:500), goat anti-rabbit IgG, Alexa Fluor 750 (ab175733, Abcam, Cambridge, UK, 1:500), goat anti-chicken IgY, Alexa Fluor 488 (A32931, 1:500, Invitrogen), goat anti-chicken IgY, Alexa Fluor 555 (A32932, Invitrogen, Waltham, MA, USA, 1:500), goat anti-chicken IgY, Alexa Fluor 750 (ab175755, Abcam, Cambridge, UK, 1:500), goat anti-mouse IgG1, Alexa 4 Fluor 88 (A21121, Invitrogen, Waltham, MA, USA, 1:500), goat anti-mouse IgG2a, Alexa Fluor 555 (A21137, Invitrogen, Waltham, MA, USA, 1:500), goat anti-mouse IgG2a, Alexa Fluor 647 (A21241, Invitrogen, Waltham, MA, USA, 1:500), goat anti-mouse IgG2b, Alexa Fluor 555 (A21147, Invitrogen, Waltham, MA, USA, 1:500), goat anti-mouse IgG2b, Alexa Fluor 647 (A21242, Invitrogen, Waltham, MA, USA, 1:500), goat anti-mouse IgM, Alexa Fluor 555 (A21426, Invitrogen, Waltham, MA, USA, 1:500), and goat anti-rat IgG, Alexa Fluor 555 (ab150158, Abcam, Cambridge, UK, 1:500).

Immunohistochemical analyses were performed as described below. After a brief wash with PBS, the sections were heated (80 °C) in 10 μM citrate buffer (pH 6) for 15 min. After another brief wash, the sections were pre-blocked in PBS containing 10% normal serum for one hour at room temperature, incubated with the relevant primary antibodies overnight at 4 °C, and then incubated with Alexa Fluor-conjugated secondary antibodies for 60 min at room temperature. The nuclei were counterstained with Hoechst 33,258. Confocal imaging was performed using an LSM980 microscope with Airyscan 2 (Zeiss).

Results

Subtypes of spiral ganglion neurons in a primate model animal, a common marmoset

First, we examined whether spiral ganglion neurons could be divided into subtypes in the common marmoset. In the Rosenthal canal of the P0 cochlea in the common marmoset, spiral ganglion neurons could be divided into PRPH-negative Type I spiral ganglion neurons and PRPH-positive Type II neurons[22]. Consistent with previous reports, CALB2 expression was observed in a part of the Type I spiral ganglion neurons at P0 cochlea in the common marmoset (Fig. 1A)[22]. In this context, we first investigated the developmental expression patterns of CALB2 in the cochlear development of the common marmoset in detail, focusing on the partial expression of CALB2 in the spiral ganglion neurons.

In the P0 cochlea, higher CALB2 expression was observed in Type I spiral ganglion neurons on the pillar side of the inner hair cells (Fig. 1B). In contrast, no CALB2 expression was detected in Type I spiral ganglion neurons on the modiolar side of the inner hair cells. Among CALB2-positive spiral ganglion neurons, neurons that were located more on the pillar side showed higher CALB2 expression than those located less on the pillar side (Fig. 1C). At this stage, no CALB2 expression was observed in Type II neurons (Fig. 1D).

Next, we investigated the expression pattern of RBFOX3, a type Ic marker, in mice[6]. In addition, we examined the intensity of the CALB2, of which expression intensity is higher in Type Ia and moderate in Ib in mice[4]. In the P0 cochlea of the common marmoset, RBFOX3 expression was detected in a part of the Type I spiral ganglion neurons ($40.0 \pm 5.8\%$); RBFOX3 expression was observed in CALB2-negative Type I spiral ganglion neurons. Our observations also revealed that the residual RBFOX3-negative and CALB2-positive Type I spiral ganglion neurons could be divided into two types depending on the intensity of CALB2 expression: CALB2-high ($32.3 \pm 3.6\%$) and CALB2-low neurons ($24.4 \pm 1.1\%$) (Fig. 1E). This observation indicates that, as reported in mice, depending on the CALB2 expression intensity and RBFOX3 expression, Type I spiral ganglion neurons in the common marmoset could also be divided into three groups (Fig. 1F).

These observations in the organ of Corti and the Rosenthal canal showed the Type I spiral ganglion neuron subtypes in this animal. These subgroups were named according to the subtypes in mice in this study. CALB2-high and RBFOX3-negative cells, which make synapses with inner hair cells on the pillar side, were named type IA in the common marmoset. Whereas, CALB2-low and RBFOX3-negative cells were named type IB. Additionally, CALB2-negative and RBFOX3-positive cells, which form synapses with inner hair cells on the modiolar side, were named type IC in the common marmoset.

Localization of CALB2-expressing spiral ganglion neurons in the organ of Corti changed during development

Next, the developmental changes in CALB2 expression in the organs of Corti were examined. A previous study investigating the cochlear development of the common marmoset mainly revealed CALB2 expression in the Rosenthal canal and described developmental expression changes of CALB2[22]. However, a detailed examination of CALB2 expression in the developing organ of Corti, especially in the distribution of CALB2-positive neurons in the organ of Corti, has not been performed. In the E120 organ of Corti, CALB2 expression was broadly observed in the spiral ganglion neurons (Fig. 2A). Notably, CALB2 expression was not restricted to around the inner hair cells, and its expression could be observed more laterally than that of pillar cells (Arrowhead in Fig. 2A). In contrast, at the E109 organ of Corti, CALB2 expression was not detected (Fig. 2B). A schematic diagram of the developmental changes in CALB2 expression in spiral ganglion neurons around the organ of Corti is shown in Fig. 2C. This observation suggests that the localization of CALB2 positive fibers occurs around E120, at the same time as the pruning of spiral ganglion neurons.

Developmental changes in RBFOX3 expression in the spiral ganglion neurons

Next, we investigated the developmental changes in RBFOX3 expression in the common marmoset (Fig. 3). RBFOX3 expression was broadly observed in the spiral ganglion neurons until E109 ($68.6 \pm 9.6\%$ at E101) (Fig. 3B and C). At E120, RBFOX3 expression was not detected in the PRPH-positive Type II neurons. However, RBFOX3 expression was still broadly detected in Type I neurons ($64.6 \pm 3.0\%$), including CLAB2-expressing cells ($45.4 \pm 4.7\%$) (Fig. 3D, * in D""). Our observations showed that the expression patterns of RBFOX3 in spiral ganglion neurons changed with the developmental stage in the cochlea. This indicates that RBFOX3 could be used as a marker of type IC spiral ganglion neurons only in the late phase of cochlear development after E120.

Initial specification of the subtypes of spiral ganglion neurons

Previous studies have suggested that the subtype specifications of Type I spiral ganglion neurons are induced by the expression of several genes, including transcription factors, before hair cell maturation[5]. In contrast, previous studies suggested that this specification depends on the electrophysiological activities of the inner hair cells[15,16]. In this study, to clarify the timing of the initial subtype specifications in the common marmoset, we examined the expression patterns of transcription factors, POU4F1 (POU domain class 4 transcription factor 1, also known as brain-specific homeobox/POU domain protein 3A (BRN3A)), TLE4 (Transducin-like enhancer of split 4), and RUNX1(Runt-related transcription factor 1, also known as acute myeloid leukemia one protein (AML1)), which have been reported as relating genes for subtype specifications in mice[5,26].

As early as E77, type I spiral ganglion neuron specifications were not observed based on the expression patterns of these transcription factors (Fig. 4A and B). TLE4 expression was not observed in spiral ganglion neurons at this stage. In contrast, POU4F1 expression was observed in all spiral ganglion neurons. Runx1 expression was not observed in spiral ganglion neurons; however, it was observed in vestibular ganglion neurons.

In E87 spiral ganglion neurons, mosaic-like expression patterns of TLE4, POU4F1, and RUNX1 were observed, indicating that initial subtype specification in the common marmoset was initiated at this point (Fig. 4C and D). Notably, at this point, hair cell development was not completed; expression of ATOH1, known

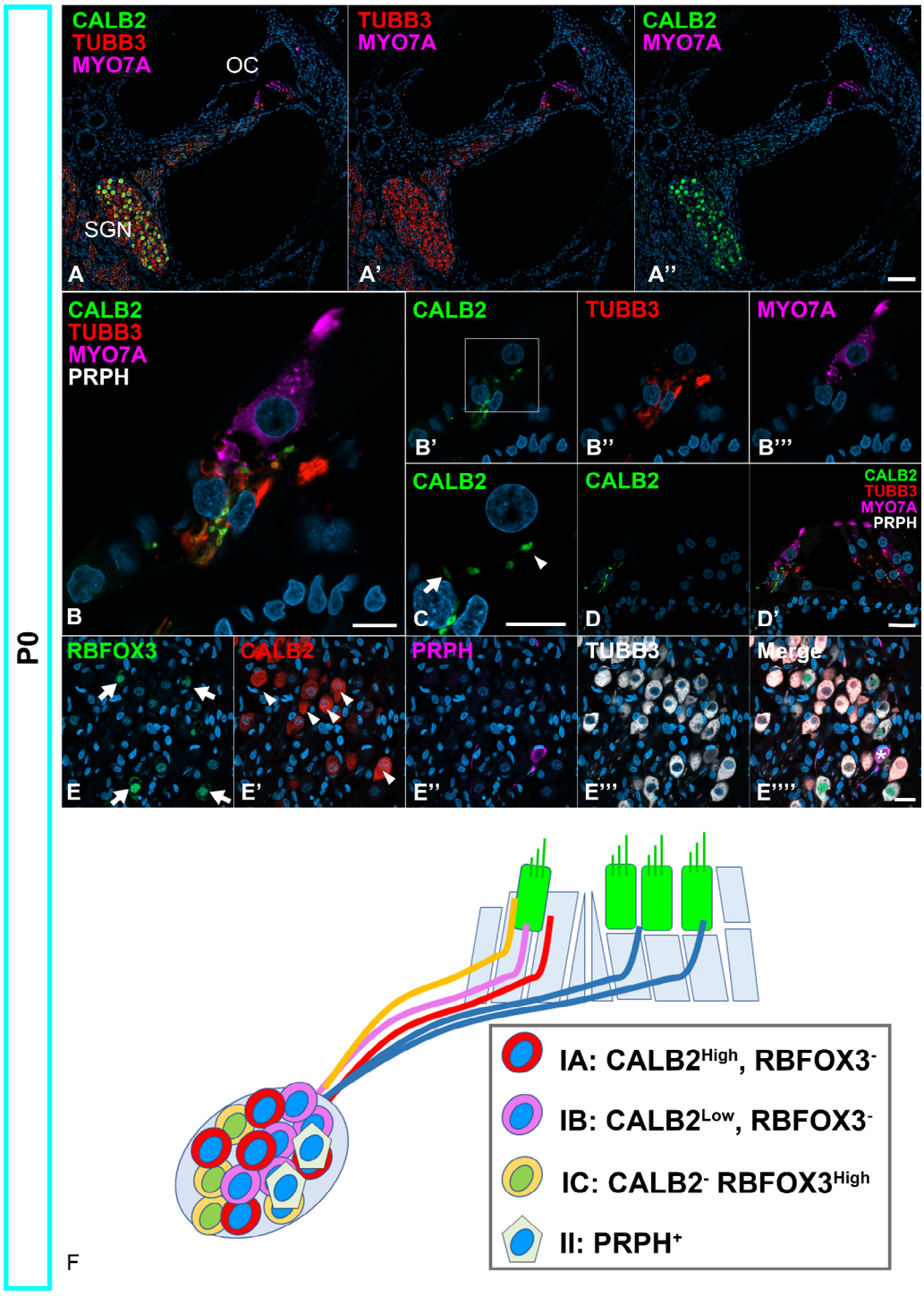

Fig. 1. Neonatal spiral ganglion neurons in the common marmoset can be divided into subtypes. (**A**) Low-magnification image of P0 cochlea. (**B**–**D**) CALB2 expression in the organ of Corti of the common marmoset. High expression of CALB2 was detected in the Type I spiral ganglion neurons located on the pillar side (Arrowhead in C); low expression of CALB2 was observed in the neurite located in the modiolar side neurite, which showed no CALB2 expression and pillar side CALB2-high neurites (Arrow in C). A higher magnification image of the bracket in A' was shown in B. No expression was observed in the PRPH-positive type II neurons (**D**). (**E**) CALB2 expression in the spiral ganglion neurons in the Rosenthal canal. At this level, CALB2 expression was observed in the part of the spiral ganglion neurons, and neurons could be subdivided into four types: CALB2 ^{High} neurons (Arrowhead in E'), CALB2 ^{Low} neurons, RBFOX3 positive neurons (Arrows in E), and PRPH positive neurons (* in E''''). (**F**) A schema of Type I spiral ganglion neuron subtypes. Spiral ganglion neurons in the common marmoset could be subdivided into Type IA, Type IB, Type IC, and Type II. The nuclei were counterstained with Hoechst (blue). Scale Bar: 100 μm in A, 10 μm in B, and C, 20 μm in D and E. SGN: spiral ganglion neurons, OC: organ of Corti.

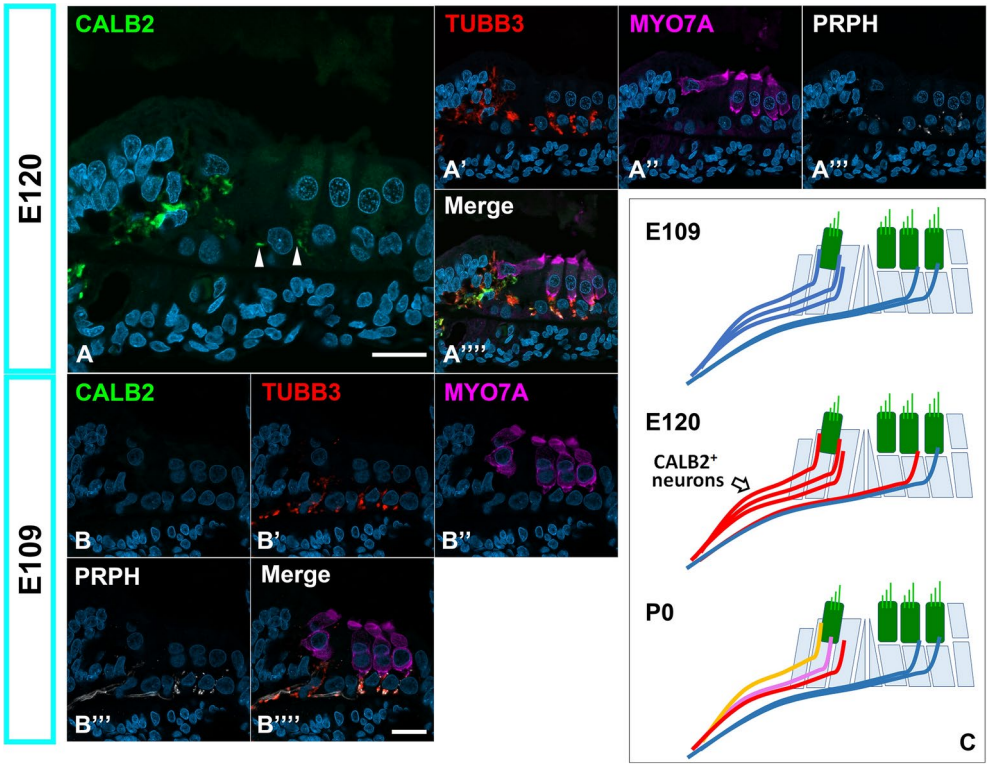

Fig. 2. Developmental changes in the expression of CALB2 in the primate organ of Corti. (**A**) Expression patterns of CALB2 in the E120 cochlea. At this stage, a broader expression of CALB2 was detected. Notably, CALB2-expressing neurite crossing the immature tunnel of Corti was observed (Arrowheads in A). (**B**) Expression patterns of CALB2 in the E109 cochlea. No expression of CLAB2 in this stage was observed in the spiral ganglion neurons around the organ of Corti. (**C**) A schema of the developmental changes in expression patterns of CALB2 in the common marmoset. CALB2 expression neurite was broadly observed in the organ of Corti at E120, and higher expression was restricted to the pillar side neurites at birth. The nuclei were counterstained with Hoechst (blue). Scale bar: 20 µm.

as an initial hair cell developmental marker[23,27], was detected in immature inner hair cells, and no specifications of outer hair cells were observed (Fig. 4E). In addition, TUBB3-positive neurites did not show obvious synapse formation between hair cells. This observation suggests that the initial subtype specifications in Type I spiral ganglion neurons could be initiated independent of the electrical activity of hair cells. Next, we examined the expression levels of these genes (Figs. 5 and 6). After E92 spiral ganglion neurons, RUNX1 expression was not detected, and POU4F1 expression was diminished (Fig. 5B). After E97, POU4F1 expression was not detected in spiral ganglion neurons (Fig. 5C). These observations indicate that the initial subtype specifications of spiral ganglion neurons occur short-term in the developmental process, before hair cell maturation or synaptic formation, which has been reported in the common marmoset at E101[22].

Expression patterns of TLE4, GATA3, and ID1 in the spiral ganglion neurons in cochlear development of the common marmoset

Next, we examined several genes (TLE4, GATA3, and ID1) whose subtype specification has been reported in rodents to clarify the inter-species similarities between rodents and primates in the differentiation of spiral ganglion neurons following initial subtype specifications (Figs. 6, 7, and 8).

Tle4 expression has been reported in Type Ia and II branches in the initial phase; however, it is limited to Type II branches in the later phase in mice[5]. In E101 and E109 in the common marmoset cochlea, TLE4 expression was detected partially in the spiral ganglion neurons, suggesting its expression in type IA and type II branches (Fig. 6A and B). In E120, TLE4 expression was restricted to the PRPH-positive Type II neurons (Fig. 6C).

Gata3 is also expressed in the Type Ia and II branches in mice[5,28,29]. Like TLE4 expression, GATA3 expression was limited to PRPH-positive type II spiral ganglion neurons until E120, while its expression was partially detected in the spiral ganglion neurons before E109 (Fig. 7).

ID1(Inhibitor of DNA Binding 1) is another gene, and its expression in the Type Ia and II branches in mice has been reported[5]. In contrast to TLE4 and GATA3, ID1 expression patterns are distinct in primates, showing differences from previous patterns reported in rodents (Fig. 8). ID1 was more broadly observed than TLE4 was in the E92 spiral ganglion neurons (Fig. 8A). During cochlear development, its expression is restricted to a part of the spiral ganglion neurons (Fig. 8B–E). However, its expression was not observed in PRPH-positive Type II

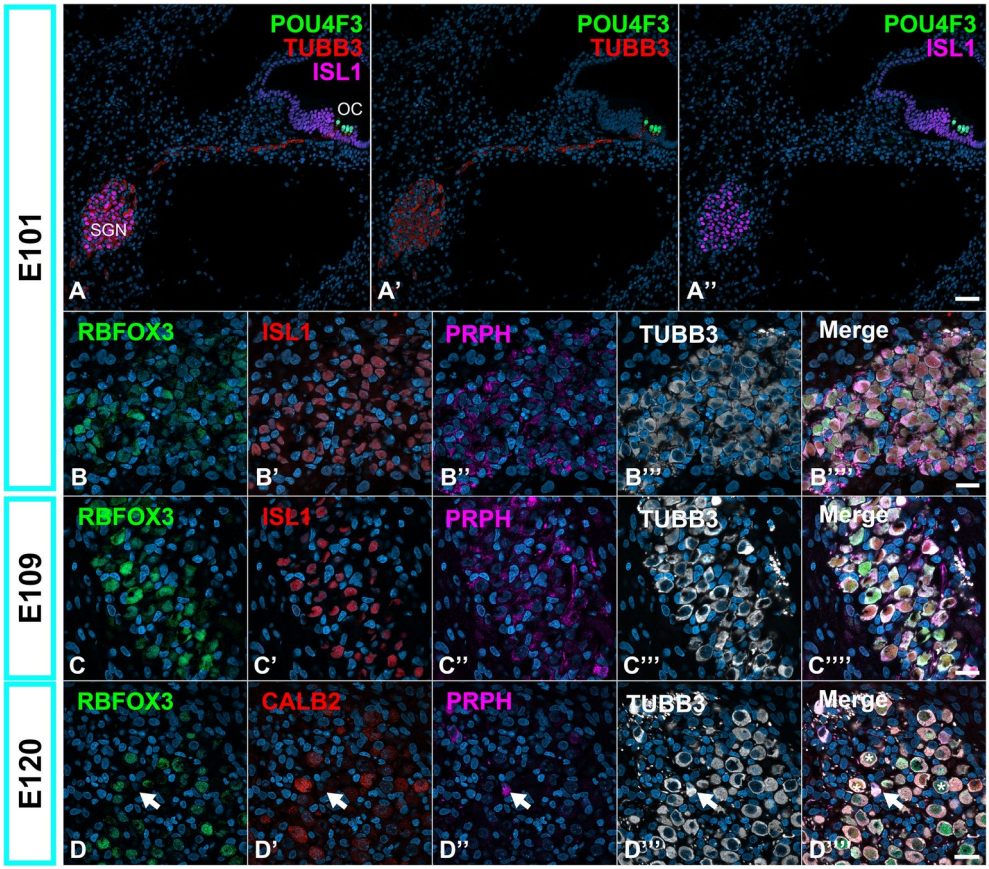

Fig. 3. Developmental changes in the expression of RBFOX3 in the primate organ of Corti. (**A**) Low-magnification image of E101 cochlea. (**B** and **C**) Expression patterns of RBFOX3 in E101 (**B**) and E109 (**C**) spiral ganglion neurons. RBFOX3 expressions were observed broadly in these stages. (**D**) Expression patterns of RBFOX3 in E120 spiral ganglion neurons. At this stage, RBFOX expression could be observed in part of Type I spiral ganglion neurons but not in type II neurons (PRPH-positive cells, Arrow in D). In this stage, RBFOX expression could also be detected in CALB2-positive cells (* in D''''). The nuclei were counterstained with Hoechst (blue). Scale bar: 50 μm in A, 20 μm in B, C and D. SGN: spiral ganglion neurons, OC: organ of Corti.

spiral ganglion neurons, suggesting that its expression is restricted to a specific part of Type I spiral ganglion neurons.

Our observations suggest that the potential for interspecies differences between rodents and primates is wider in the subsequent stages than in the initial specification stage of cochlear development, at least in the Type Ia and Type II branches.

Expression patterns of TTN, NCALD, TRIM54, and INA in the spiral ganglion neurons in the cochlear development of the common marmoset

Finally, we examined the expression of other subtype-specific genes in mature spiral ganglion neurons reported in mice, namely TRIM54, TTN, NCALD, and INA (Fig. 9). Previous studies have revealed the subtype-specific expression of several genes, whereas the expression of *Trim54*, *Ttn*, and *Ncald* is specific for Ia, Ib, and Ic, respectively. The *Ina* expression has been reported to follow an Ia > Ib > Ic gradient. In this study, we examined the expression patterns of these genes[4,16].

In the P0 cochlea of the common marmoset, TRIM54 expression was observed only in PRPH-positive type II spiral ganglion neurons (Fig. 9A). TRIM54 expression was not observed until E120. TTN expression was first detected in E120 spiral ganglion neurons, where TTN expression was broadly observed in both Type I and Type II neurons (Fig. 9B). This broader expression was also observed in P0 cochlea (Fig. 9C). The localization of TTN expression in specific subtypes of Type I spinal ganglion neurons was not detected in the common marmoset. NCALD expression was first detected in P0 spiral ganglion neurons, whereas NCALD expression was broadly observed in Type I but not detected in Type II spiral ganglion neurons (Fig. 9D). Localization of NCALD in specific subtypes of Type I spinal ganglion neurons was not detected in the common marmoset. In the P0 cochlea of the common marmoset, INA expression was observed only in PRPH-positive type II spiral ganglion neurons (Fig. 9E). INA expression was not observed until E120. This characteristic gradient of INA

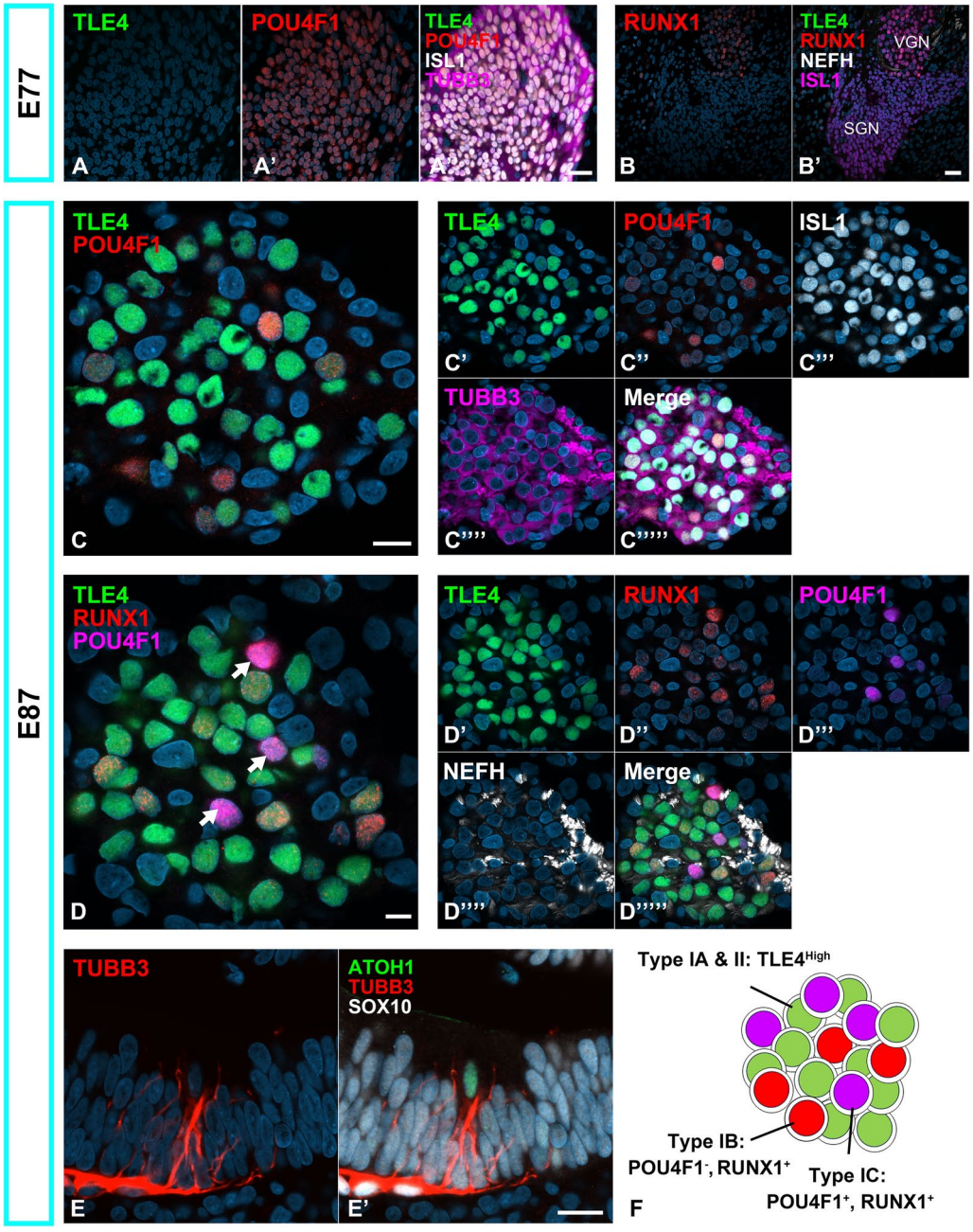

Fig. 4. Expression patterns of TLE4, POU4F1, and RUNX1 in E77 and E87 cochlea. (**A** and **B**) TLE4, POU4F1, and RUNX1 expression patterns in E77 spiral ganglion neurons. TLE4 and RUNX4 expressions in this stage were not observed in spiral ganglion neurons. In contrast, at this stage, POU4F1 expressions were observed broadly in spiral ganglion neurons. (**C** and **D**) The TLE4, POU4F1, and RUNX1 expression patterns in 87 spiral ganglion neurons. At this stage, distinct TLE4, POU4F1, and RUNX1 expression could be observed in part of Type I spiral ganglion neurons; highly TLE4-positive cells showed no POU4F1 and RUNX1 expressions, and expression of POU4F1 was observed in a part of RUNX1 positive cells (Arrows in D). (**E**) Development of the organ of Corti at this stage. ATOH1-positive cells were only observed in developing inner hair cell regions, and no mature hair cells or synapses were observed. (**F**) A schema showing expression patterns in spiral ganglion neurons at this stage. The nuclei were counterstained with Hoechst (blue). SGN: spiral ganglion neuron, VGN: vestibular ganglion neuron. Scale bar: 20 μm in A, B and E, 10 μm in C and D.

expression among subtypes of Type I spinal ganglion neurons reported in mice[4] has not been detected in the common marmoset.

A schematic diagram of the spatiotemporal expression patterns of the genes examined in this study is shown in Fig. 10.

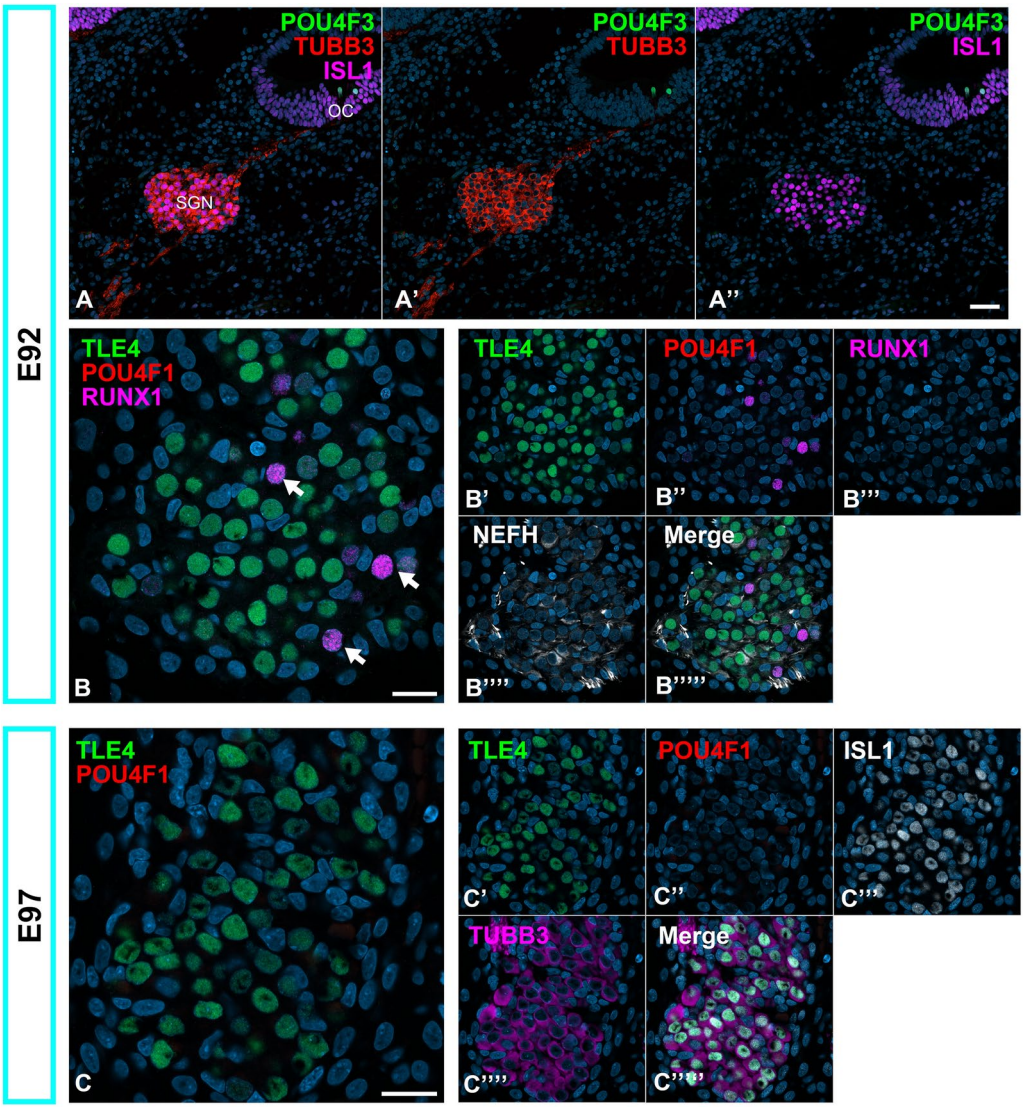

Fig. 5. Developmental changes in the expression of POU4F1 and RUNX1 in the spiral ganglion neurons. (**A**) Low-magnification image of E92 cochlea. (**B**) Expression patterns of POU4F1 and RUNX1 in E92 spiral ganglion neurons. At this stage, POU4F1 expression was observed in several cells (Arrows in B), while RUNX1 expression was diminished. (**C**) Expression patterns of POU4F1 and RUNX1 in E97 spiral ganglion neurons. At this stage, POU4F1 expressions have not been observed. In E92 and E97, TLE4 expression observed in a part of spiral ganglion neurons has remained. The nuclei were counterstained with Hoechst (blue). Scale bar: 50 μm in A, 20 μm in B and C. SGN: spiral ganglion neurons, OC: organ of Corti.

Discussion

Type I spiral ganglion neurons in the common marmoset are also divided into subtypes

This study revealed that the Type I spiral ganglion neurons could also be subdivided into at least three subtypes in primates based on their gene expression patterns, as previously reported in mice[1,2,30]. So far, subtype-specification of the spiral ganglion neurons and developmental studies investigating the mechanisms of these specifications have been mainly performed using fetuses or newborns of the mice. Comprehensive gene expression analyses using single-cell RNA sequencing have led to significant progress in this field. In contrast to mice, primate investigations have not been performed, despite the reported interspecies differences in cochlear development between rodents and primates[19,20]. To our knowledge, this is the first report addressing the identification of subtypes of the Type I spiral ganglion neurons in cochlear development in primates.

Gene expression patterns at the initial subtype specification of the spiral ganglion neurons in common marmosets are similar to those in rodents

We examined the time point of initiation of spiral ganglion neuron sub-specification in cochlear development in the common marmoset by investigating the early expression patterns of the genes reported as marker molecules for specifications of Type I spiral ganglion neurons in mice: *TLE4*, *POU4F1*, and *RUNX1*[5,31]. As shown in Fig. 4F,

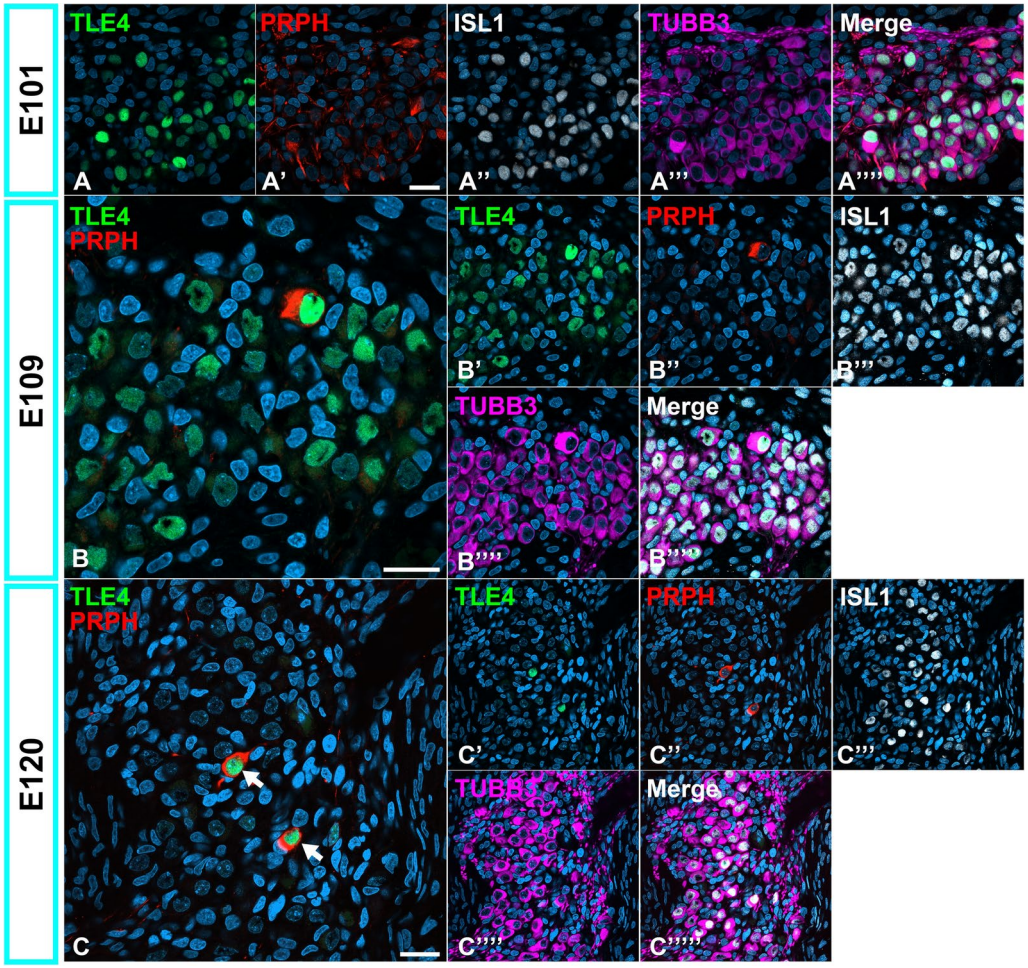

Fig. 6. Developmental changes in the expression of TLE4 in the spiral ganglion neurons. (**A** and **B**) Expression patterns of TLE4 in E101 (**A**) and E109 (**B**) spiral ganglion neurons. At this stage, TLE4 expression was still observed in a part of spiral ganglion neurons. (**C**) Expression patterns of TLE4 in E120 spiral ganglion neurons. At this stage, TLE4 expression was restricted to PRPH-positive Type II spiral ganglion neurons (Arrows in C), suggesting that the expression of TLE4 in Type IA spiral ganglion neurons has been diminished until this stage. The nuclei were counterstained with Hoechst (blue). Scale bar: 20 µm.

a schema of E87 spiral ganglion neurons, the expression patterns of these three genes were well preserved between rodents and common marmosets, suggesting early subtype specification in the common marmoset: TLE4 high in Types IA and II, POU4F1-negative and RUNX1-positive in Type IB, and POU4F1-positive and RUNX1-positive in Type IC.

Notably, these sequential gene expression patterns are also well preserved in both rodents and primates. As previously reported by Sanders et al., Type Ib and Ic is suggested to be the default type of spiral ganglion neurons. Additionally, they proposed that Type Ia and II would require additional developmental cues, based on their observations. Specific gene expression of type Ia and II branches is observed exclusively in these cells. In contrast, type Ib- and Ic-specific genes are broadly observed initially; however, they become restricted as developmental stages progress in the early phase[5]. These similarities in our observation of the common marmoset suggest the possibility that type IB and IC branches are the default mode of Type I spiral ganglion neurons in primates in the same way as mice. Therefore, a detailed examination of these aspects is required.

Steps of subtype-specification of spiral ganglion in the common marmoset could be divided into two stages: before and after hair cell maturation

Our observations indicate that the process of subtype-specification of the spiral ganglion neurons can be divided into two stages by hair cell maturation. The first step involves observing mosaic-like expression patterns in spiral ganglion neurons, which precede hair cell maturation. These patterns could be observed among the morphologically homogenous developmental premature spiral ganglion neurons. This initial sub-specification could be observed as a difference in *TLE4, POU4F1*, and *RUNX1* gene expression patterns. Specific synaptic formation with hair cells could not be observed at this stage, indicating that this process is independent of the electrical activity of hair cells but is controlled by developmental cascades of gene expression.

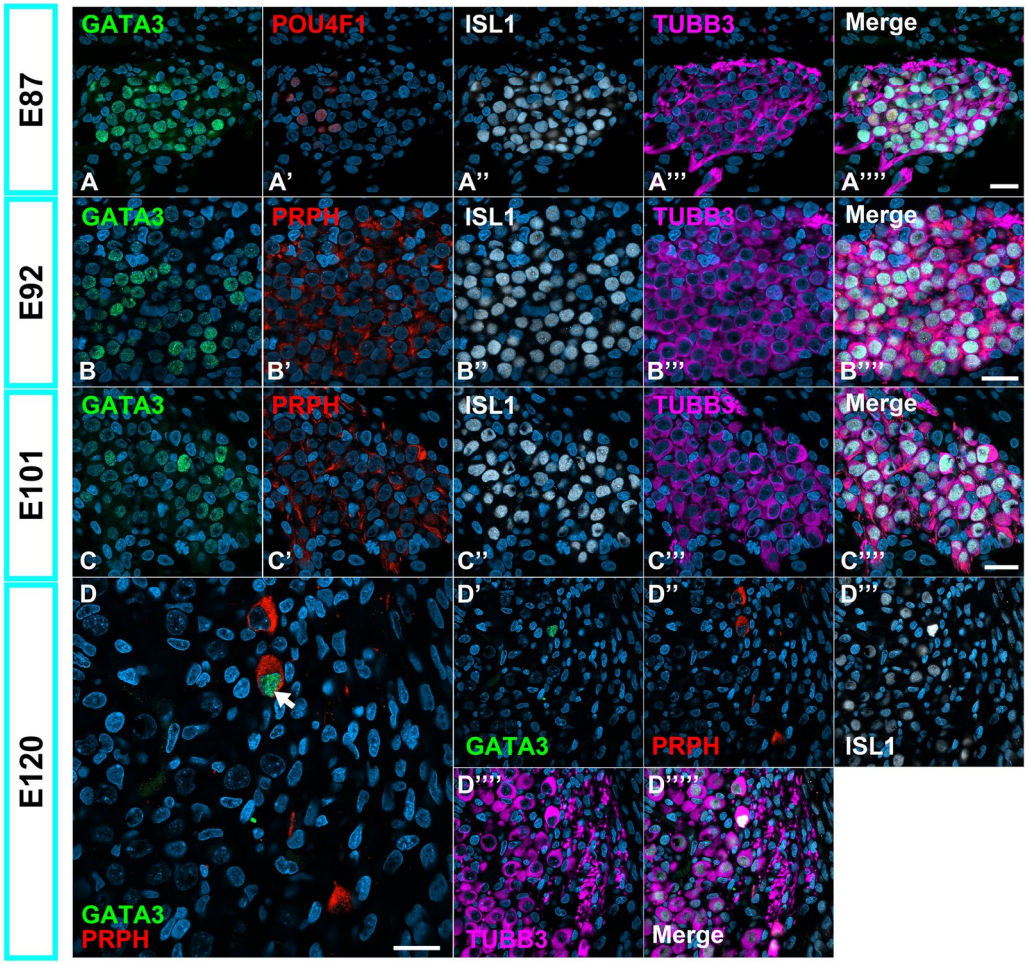

Fig. 7. Developmental changes in the expression of GATA3 in the spiral ganglion neurons. (**A**) Expression patterns of GATA3 in E87 spiral ganglion neurons. At this stage, GATA3 expression was observed in the POU4F1-negative spiral ganglion neurons. (**B** and **C**) Expression patterns of GATA3 in the E92(B) and E101(B) cochlea. At these stages, GATA3 expressions were detected in a part of spiral ganglion neurons. (**D**) Expression patterns of GATA3 in the E120 spiral ganglion neurons. At this stage, GATA3 expressions have been restricted to PRPH-positive Type II spiral ganglion neurons (Arrow in D), suggesting that the expression of GATA3 in Type IA spiral ganglion neurons has been diminished until this stage. The nuclei were counterstained with Hoechst (blue). Scale bar: 20 μm.

The second step is the formation for specific spatial patterns of each subtype after hair cell maturation and synaptic formation, in agreement with the pruning of the spiral ganglion neurons. Previous reports showed that until this pruning step, hair cells and initial synaptic formation were completed[22], followed by stria vascularis and lateral wall fibrocyte maturation[32,33], which is essential for establishing the endocochlear potential. Thus, this pruning is thought to depend on the electrical activity of hair cells in the common marmoset. Our observations suggest that the second step, observed as pruning, could also depend on the electrical activity of hair cells.

Our observations indicate that both early induction by specific gene expression and late modifications depending on electrical activity are essential for normal differentiation of the subtypes of Type I spiral ganglion neurons in the common marmoset. To date, two theories have been suggested based on observations in rodents, and whether sub-specification of Type I spiral ganglion neurons is dependent or independent of the electrical activities of hair cells has not been concluded[5,15,16]. Our observation in the common marmoset, where the developmental process proceeds three times more slowly, is suitable for detecting spatiotemporal steps in cochlear development[19,23]. These findings are compatible with previous observations in rodents. This slow growth rate was suitable for distinguishing between the two steps. The first step precedes the second by more than 30 days in the common marmoset, which is sufficient to distinguish these steps clearly. Our observations suggest that both steps are essential for the subtype-specification of spiral ganglion neurons. This observation suggests the usefulness of the common marmoset as a tool for studying cochlear development.

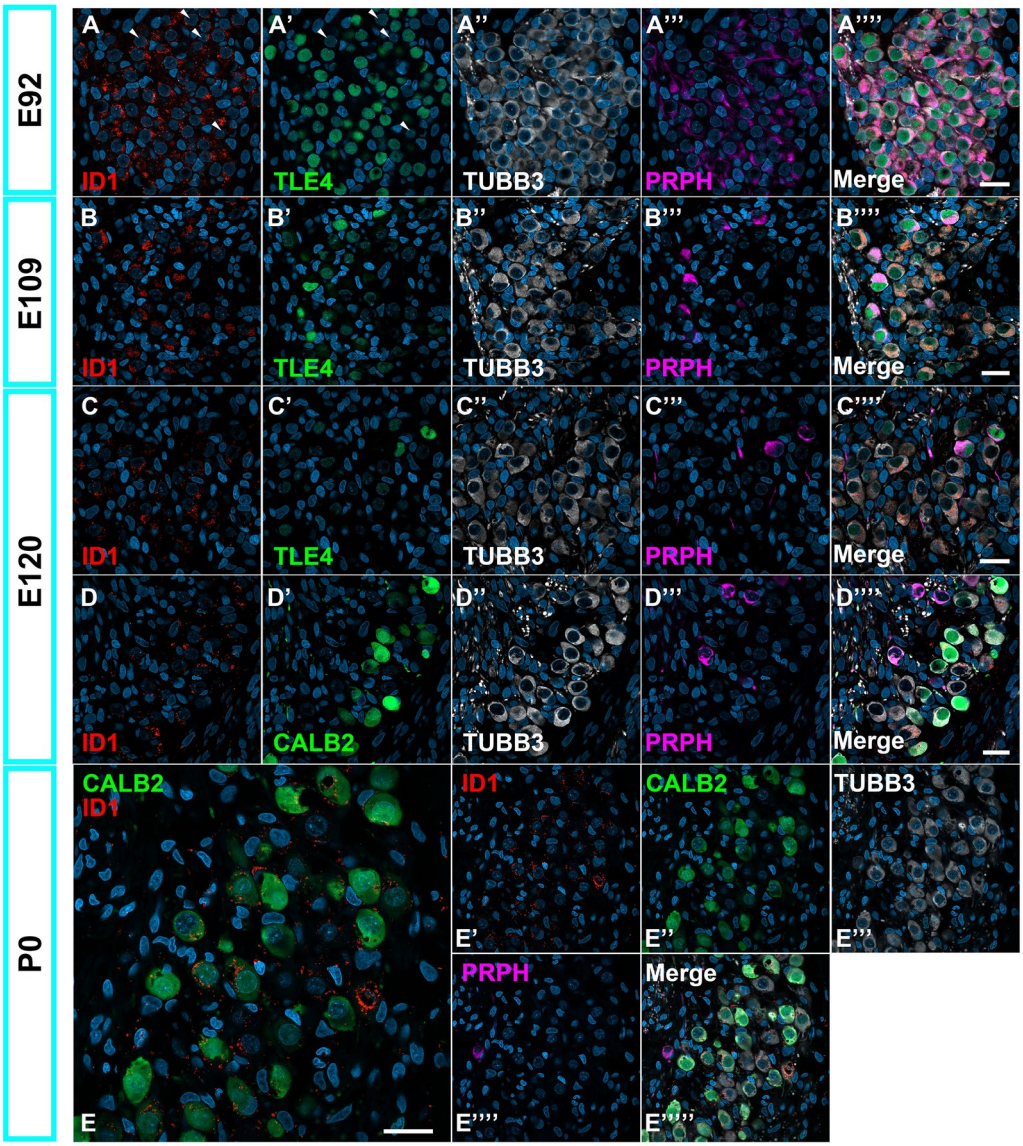

Fig. 8. Developmental changes in the expression of ID1 in the spiral ganglion neurons. (**A**) ID1 expression in E92 spiral ganglion neurons. ID1 is more broadly observed at this stage than TLE4 is (Arrowhead in A). (**B**–**D**) ID1 expression in E109 (**B**) and E120 (**C** and **D**) spiral ganglion neurons. At these stages, ID1 expression was observed in Type I and II spiral ganglion neurons. In Type I spiral ganglion neurons, ID1 expression was observed in TLE4-negative or CALB2-negative cells. (**E**) ID1 expression in D0 cochlea. ID1 expression was observed in Type I spiral ganglion neurons and not detected in PRPH-positive Type II spiral ganglion neurons. The nuclei were counterstained with Hoechst (blue). Scale bar: 20 µm.

Following gene expression patterns after initial specification, similarities and differences between the common marmoset and rodents were observed

After the initial specifications of the spiral ganglion neurons, we analyzed the following gene expression patterns, focusing on the Type Ia and II branches: GATA3 and ID1[5]. Moreover, we investigated mature subtype-specific markers of spiral ganglion neurons in common marmosets: TRIM54, TTN, NCALD, and INA[6,16].

While *Gata3*, *Id1,* and *Tle4* expression was specific to Type Ia and II branches in mice[5,34], developmental expression patterns of these genes in the cochlea of the common marmoset showed significant differences. Our observations showed that the developmental changes in GATA3 expression were well-preserved between mice and the common marmoset. Another type of Ia- and II-specific gene, TLE4, was also preserved. In contrast, ID1 showed characteristic expression patterns in the common marmoset; ID1 expression was broadly observed in Type I spiral ganglion neurons.

These observations support the idea that most gene expression patterns in the early initiation of sub-specification of Type I spiral ganglion neurons are preserved in the common marmoset and rodent. In contrast, the present study revealed that the common marmoset does not always preserve subtype-specific gene expression patterns in the mature Type I spiral ganglion neurons in mice. Combined with the preservative expression

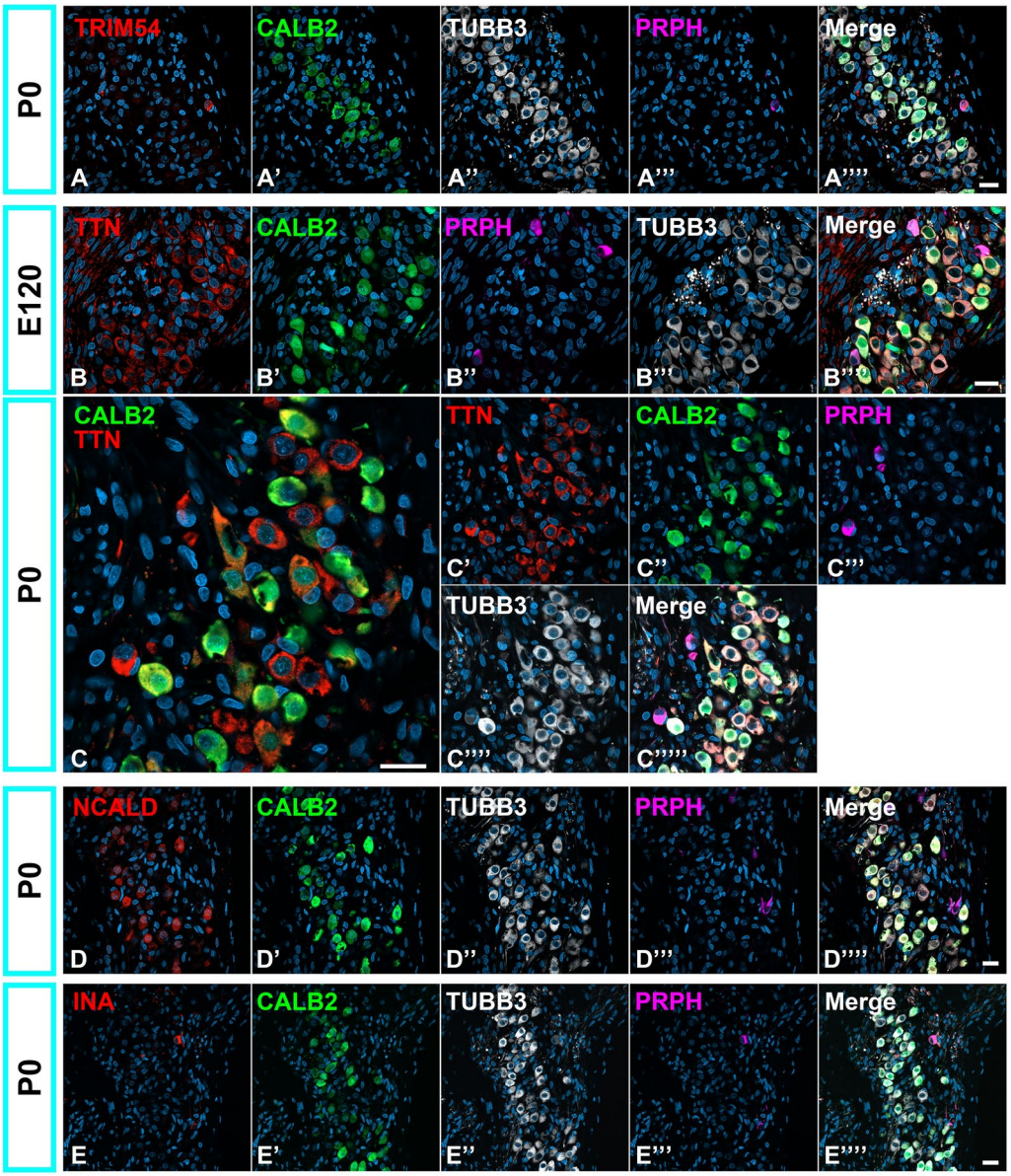

Fig. 9. Expression patterns of TRIM54, TTN, NCALD, and INA in the spiral ganglion neurons. (**A**) Expression pattern of TRIM54 in the spiral ganglion neuron. TRIM54 was observed in PRPH-positive Type II spiral ganglion neurons at P0 cochlea; no expression was detected in Type I spiral ganglion neurons. (**B** and **C**) Expression pattern of TTN in spiral ganglion neuron in E120 and P0 spiral ganglion neurons. In E120, TTN expression was broadly observed in spiral ganglion neurons. Its expression was detected in both Type I and II neurons. In P0 spiral ganglion neurons, still-board TTN expression could be detected in both Type I and II spiral ganglion neurons. (**D**) Expression pattern of NCALD in the spiral ganglion neuron. NCALD expression was broadly observed in Type I spiral ganglion neurons at P0 cochlea, and no expression was detected in PRPH-positive type II spiral ganglion neurons. (**E**) Expression pattern of INA in the spiral ganglion neuron. INA expression is observed in PRPH-positive Type II spiral ganglion neurons at P0 cochlea, and no expression was detected in Type I spiral ganglion neurons. The nuclei were counterstained with Hoechst (blue). Scale bar: 20 μm.

patterns of the initial gene expression patterns of the subtype-specification and the discrepancies observed in the common marmoset, these similarities and discrepancies between mice and the common marmoset would suggest that maturation and the subsequent developmental process differ between these species.

Supporting this observation, mature subtype-specific markers known in mice showed several discrepancies. For example, although Ttn is known as one of the Type Ib spiral ganglion neurons in mice and for its limited expression to this type[4,16], its expression was broadly observed in the Type I spiral ganglion neurons in primates. This discrepancy suggests that the initial developmental signaling is preserved between rodents and primates; however, the developed Type I spiral ganglion neurons have different characteristics. A future, detailed study

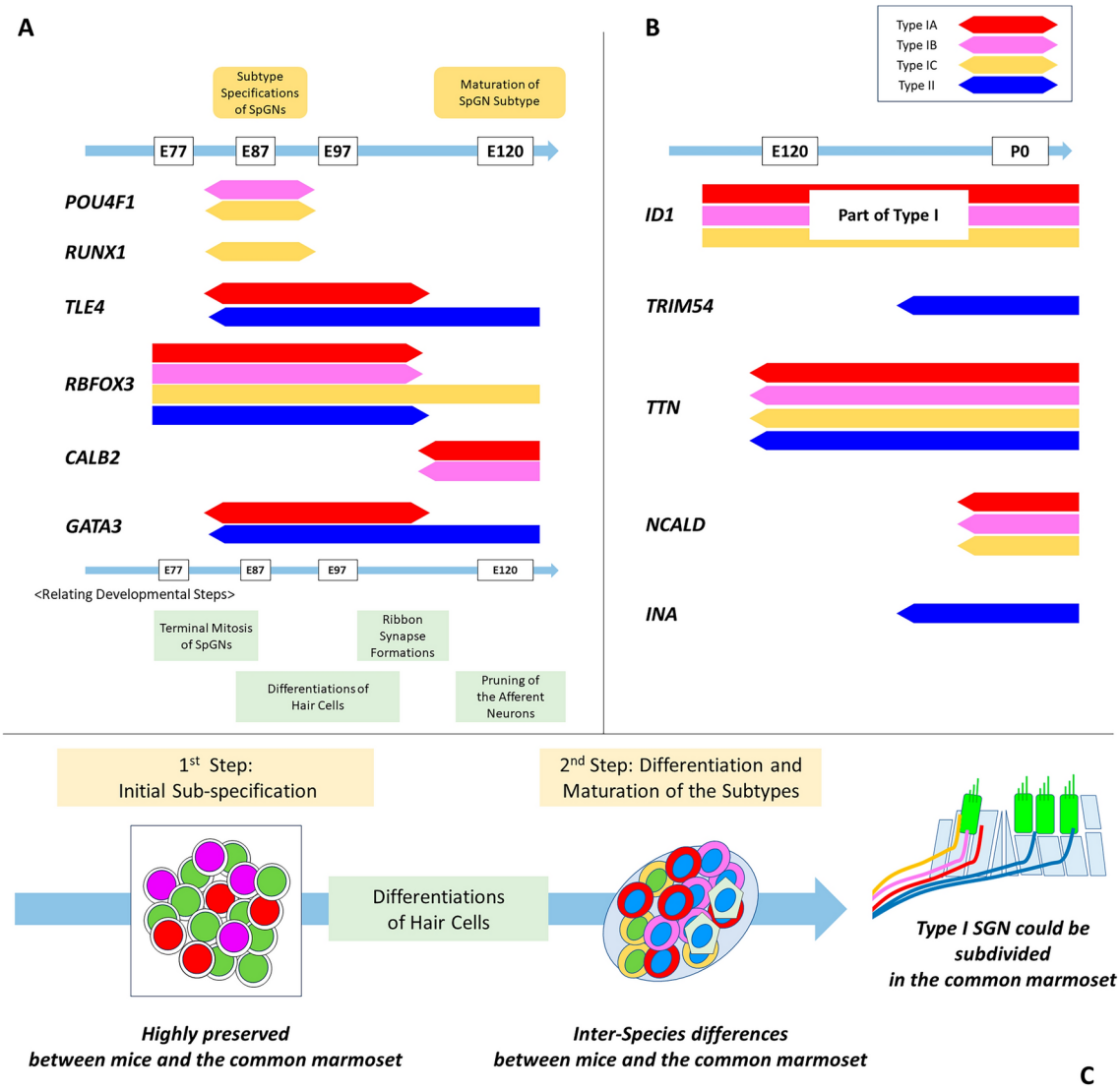

Fig. 10. Schematic Diagram of subtype specifications of the spiral ganglion neurons in the common marmoset. (**A**) The spatiotemporal expression patterns of POU4F1, RUNX1, TLE4, RBFOX3, CALB2 and GATA3 are shown, comparing related developmental steps in the cochlea of the common marmoset. Subtype specifications in the spiral ganglion neurons precede the differentiation of hair cells and ribbon synapse formations. Maturation of each subtype occurs with pruning of the spiral ganglion neurons. (**B**) The spatiotemporal expression patterns of ID1, TRIM54, TTN, NCALD, and INA are shown. Our observations revealed several similarities and inter-species differences between rodent and primate subtype-specific gene expression patterns. (**C**) Steps of subtype-specification of spiral ganglion in the common marmoset could be divided into two stages: before and after hair cell maturation. Our observations indicate that the earlier stage of subtype specification was highly preserved between rodents and the common marmoset, while the subsequent differentiation of the subtypes and maturation of the spiral ganglion neurons demonstrated several inter-species differences. SGN: Spiral ganglion neurons.

would help to clarify this point. At the same time, our observations suggest that careful attention is required when applying our understanding obtained from rodents to humans.

Importance of investigating the subtypes in spiral ganglion neurons in the primate model animal

Moreover, these subtypes of Type I spiral ganglion neurons are clinically important, especially from the viewpoint of cochlear synaptopathy and hidden hearing loss[35,36]. It has been speculated that differences in neuroelectric characteristics among the subtypes of the spiral ganglion neurons result in greater dynamic ranges of the neuronal activity evoked from the inner hair cells. It has also been assumed that this dynamic range could diminish with aging or acoustic trauma, as the diversity of this subtype is lost. Type Ia neurons are more vulnerable to aging than type Ic neurons are[37–39]. Therefore, understanding the subtypes and the specification mechanisms is also

important from a clinical viewpoint as well as developing treatment in the future. Our observations show the potential importance of investigating primate animal models for age-related hearing loss or hidden hearing loss.

Limitations of this study

In this study, we performed immunohistological analysis using a primate model animal to investigate the similarities and differences in cochlear development between rodents and the common marmoset from the viewpoint of subtype specifications of the spiral ganglion neuron. Gene expression patterns and specificities in subtypes of the spiral ganglion neurons have been investigated in comprehensive analyses, such as single-cell RNA sequencing in mice. However, the application of these technologies to primate cochlear development has not yet been established. Thus, investigations in this study had to be only performed using selected markers. Therefore, we also need to follow future comprehensive analyses of the development of common marmoset cochlea.

Conclusion

This study revealed that Type I spiral ganglion neurons could also be subdivided into at least three subtypes in primates based on their gene expression patterns, as previously reported in rodents. We also clarified the important developmental time points for the initial differentiation of subtypes in the spiral ganglion neurons and their subsequent maturation in the common marmoset. In addition, we revealed several interspecies differences between rodents and the common marmoset by comparing previous reports on rodents with the present study. Our observations indicate that the earlier stage of subtype specification was highly preserved between rodents and the common marmoset. However, the subsequent differentiation of the subtypes and maturation of the spiral ganglion neurons demonstrated several inter-species differences. Our results suggest the necessity and usefulness of primate-specific knowledge regarding subtype specifications in spiral ganglion neurons. The time course established in this study will aid in studying the primate-specific developmental biology of the inner ear. This could eventually lead to new treatment strategies for hearing loss in humans. Moreover, understanding the differences and similarities in the subtype specifications in the spiral ganglion neurons would be valuable for studying age-related hearing loss as well as designing regenerative therapies.

Data availability

The datasets used and analyzed during the current study available from the corresponding author on reasonable request.

Received: 24 May 2024; Accepted: 17 October 2024
Published online: 24 October 2024

References

1. Kiang, N. et al. Afferent innervation of the mammalian cochlea. In *Comparative physiology of sensory systems* (eds Keynes, R. D. & Maddrell, S. H. P.) 143–161 (Cambridge University Press, 1984).
2. Nayagam, B. A., Muniak, M. A. & Ryugo, D. K. The spiral ganglion: Connecting the peripheral and central auditory systems. *Hear. Res.* **278**, 2–20 (2011).
3. Liberman, M. C. Single-neuron labeling in the cat auditory nerve. *Science* **216**, 1239–1241. https://doi.org/10.1126/science.7079757 (1982).
4. Petitpre, C. et al. Neuronal heterogeneity and stereotyped connectivity in the auditory afferent system. *Nat. Commun.* **9**, 3691. https://doi.org/10.1038/s41467-018-06033-3 (2018).
5. Sanders, T. R. & Kelley, M. W. Specification of neuronal subtypes in the spiral ganglion begins prior to birth in the mouse. *Proc. Natl. Acad. Sci.* **119**, e2203935119 (2022).
6. Petitpre, C. et al. Single-cell RNA-sequencing analysis of the developing mouse inner ear identifies molecular logic of auditory neuron diversification. *Nat. Commun.* **13**, 3878. https://doi.org/10.1038/s41467-022-31580-1 (2022).
7. Liberman, M. C. Noise-induced and age-related hearing loss: New perspectives and potential therapies. *F1000Res* **6**, 927. https://doi.org/10.12688/f1000research.11310.1 (2017).
8. Moser, T., Karagulyan, N., Neef, J. & Tobón, L. M. J. Diversity matters - extending sound intensity coding by inner hair cells via heterogeneous synapses. *Embo J.* **42**, e114587. https://doi.org/10.15252/embj.2023114587 (2023).
9. Kiang, N. Y., Watanabe, T., Thomas, E. C. & Clark, L. F. *Discharge patterns of single fibers in the cat's auditory nerve* (M.I.T. Press, 1966).
10. Sachs, M. B. & Abbas, P. J. Rate versus level functions for auditory-nerve fibers in cats: Tone-burst stimuli. *J. Acoust. Soc. Am.* **56**, 1835–1847. https://doi.org/10.1121/1.1903521 (1974).
11. Liberman, M. C. Auditory-nerve response from cats raised in a low-noise chamber. *J. Acoust. Soc. Am.* **63**, 442–455. https://doi.org/10.1121/1.381736 (1978).
12. Borg, E., Engstrom, B., Linde, G. & Marklund, K. Eighth nerve fiber firing features in normal-hearing rabbits. *Hear Res.* **36**, 191–201. https://doi.org/10.1016/0378-5955(88)90061-5 (1988).
13. Jackson, B. S. & Carney, L. H. The spontaneous-rate histogram of the auditory nerve can be explained by only two or three spontaneous rates and long-range dependence. *Jaro* **6**, 148–159. https://doi.org/10.1007/s10162-005-5045-6 (2005).
14. Heil, P. & Peterson, A. J. Basic response properties of auditory nerve fibers: A review. *Cell Tissue Res.* **361**, 129–158. https://doi.org/10.1007/s00441-015-2177-9 (2015).
15. Sun, S. et al. Hair cell mechanotransduction regulates spontaneous activity and spiral ganglion subtype specification in the auditory system. *Cell* **174**(1247–1263), e1215. https://doi.org/10.1016/j.cell.2018.07.008 (2018).
16. Shrestha, B. R. et al. Sensory neuron diversity in the inner ear is shaped by activity. *Cell* **174**(1229–1246), e1217. https://doi.org/10.1016/j.cell.2018.07.007 (2018).
17. Siebald, C. et al. Molecular signatures define subtypes of auditory afferents with distinct peripheral projection patterns and physiological properties. *Proc. Natl. Acad. Sci. USA* **120**, e2217033120. https://doi.org/10.1073/pnas.2217033120 (2023).
18. Locher, H. et al. Neurosensory development and cell fate determination in the human cochlea. *Neural Dev.* **8**, 20. https://doi.org/10.1186/1749-8104-8-20 (2013).
19. Hosoya, M., Fujioka, M., Murayama, A. Y., Okano, H. & Ogawa, K. The common marmoset as suitable nonhuman alternative for the analysis of primate cochlear development. *FEBS J.* **288**, 325–353. https://doi.org/10.1111/febs.15341 (2021).

20. Hosoya, M., Fujioka, M., Ogawa, K. & Okano, H. Distinct expression patterns of causative genes responsible for hereditary progressive hearing loss in non-human primate cochlea. *Sci. Rep.* **6**, 22250. https://doi.org/10.1038/srep22250 (2016).
21. Grandi, F. C., De Tomasi, L. & Mustapha, M. Single-cell RNA analysis of type I spiral ganglion neurons reveals a Lmx1a population in the cochlea. *Front. Mol. Neurosci.* **13**, 83. https://doi.org/10.3389/fnmol.2020.00083 (2020).
22. Hosoya, M. et al. Neuronal development in the cochlea of a nonhuman primate model, the common marmoset. *Dev. Neurobiol.* **81**, 905–938. https://doi.org/10.1002/dneu.22850 (2021).
23. Hosoya, M. et al. Early development of the cochlea of the common marmoset, a non-human primate model. *Neural Dev.* **17**, 6. https://doi.org/10.1186/s13064-022-00162-8 (2022).
24. Hosoya, M. et al. Distribution of macrophages in the developing cochlea of the common marmoset, a primate model animal. *Front. Immunol.* **14**, 1229414. https://doi.org/10.3389/fimmu.2023.1229414 (2023).
25. Murayama, A. Y. et al. The polymicrogyria-associated GPR56 promoter preferentially drives gene expression in developing GABAergic neurons in common marmosets. *Sci. Rep.* **10**, 21516. https://doi.org/10.1038/s41598-020-78608-4 (2020).
26. Sherrill, H. E. et al. Pou4f1 defines a subgroup of type I spiral ganglion neurons and is necessary for normal inner hair cell presynaptic Ca2+ signaling. *J. Neurosci.* **39**, 5284–5298 (2019).
27. Woods, C., Montcouquiol, M. & Kelley, M. W. Math1 regulates development of the sensory epithelium in the mammalian cochlea. *Nat. Neurosci.* **7**, 1310–1318 (2004).
28. van der Wees, J. et al. Hearing loss following Gata3 haploinsufficiency is caused by cochlear disorder. *Neurobiol. Dis.* **16**, 169–178. https://doi.org/10.1016/j.nbd.2004.02.004 (2004).
29. Luo, X. J. et al. GATA3 controls the specification of prosensory domain and neuronal survival in the mouse cochlea. *Hum. Mol. Genet.* **22**, 3609–3623. https://doi.org/10.1093/hmg/ddt212 (2013).
30. Barclay, M., Ryan, A. F. & Housley, G. D. Type I vs type II spiral ganglion neurons exhibit differential survival and neuritogenesis during cochlear development. *Neural Dev.* **6**, 1–14 (2011).
31. Shrestha, B. R., Wu, L. & Goodrich, L. V. Runx1 controls auditory sensory neuron diversity in mice. *Dev. Cell* **58**(306–319), e305 (2023).
32. Hosoya, M. et al. Development of cochlear spiral ligament fibrocytes of the common marmoset, a nonhuman model animal. *Sci. Rep.* **13**, 11789. https://doi.org/10.1038/s41598-023-39003-x (2023).
33. Hosoya, M. et al. Development of the stria vascularis in the common marmoset, a primate model. *Sci Rep* **12**, 19811. https://doi.org/10.1038/s41598-022-24380-6 (2022).
34. Nishimura, K., Noda, T. & Dabdoub, A. Dynamic expression of Sox2, Gata3, and Prox1 during primary auditory neuron development in the mammalian cochlea. *PLoS One* **12**, e0170568. https://doi.org/10.1371/journal.pone.0170568 (2017).
35. Moser, T., Predoehl, F. & Starr, A. Review of hair cell synapse defects in sensorineural hearing impairment. *Otol Neurotol* **34**, 995–1004. https://doi.org/10.1097/MAO.0b013e3182814d4a (2013).
36. Kujawa, S. G. & Liberman, M. C. Synaptopathy in the noise-exposed and aging cochlea: primary neural degeneration in acquired sensorineural hearing loss. *Hear. Res.* **330**, 191–199. https://doi.org/10.1016/j.heares.2015.02.009 (2015).
37. Wang, M., Lin, S. & Xie, R. Apical-basal distribution of different subtypes of spiral ganglion neurons in the cochlea and the changes during aging. *Plos one* **18**, e0292676 (2023).
38. Schmiedt, R. A., Mills, J. H. & Boettcher, F. A. Age-related loss of activity of auditory-nerve fibers. *J. Neurophys.* **76**, 2799–2803. https://doi.org/10.1152/jn.1996.76.4.2799 (1996).
39. Sergeyenko, Y., Lall, K., Liberman, M. C. & Kujawa, S. G. Age-related cochlear synaptopathy: an early-onset contributor to auditory functional decline. *J. Neurosci.* **33**, 13686–13694 (2013).

Acknowledgements

We thank Saki Ninomiya for providing technical support. We thank Ayako Y. Murayama, Sho Yoshimatsu, Junko Okahara and Hideyuki Okano for providing materials.

Author contributions

M.H., M.U., M.S., T.N., N.O., H.O., conceived and designed the experiments. M.H. and M.U., wrote the manuscript. M.H. performed most of the experiments. M.H., M.U., and M.S. analyzed the data. All authors read and approved the final version of the manuscript.

Funding

MH was supported by a grant from the Japanese government, MEXT KAKENHI (Grant-in-Aid for Scientific Research (B) 20H03836, Grant-in-Aid for Challenging Research (Exploratory) 21K19581, Grant-in-Aid for Scientific Research (C) 24K12727), the Keio Medical Association, and Keio University Medical Science Fund, and Keio Gijuku Academic Development Funds. MS was supported by a grant from Japanese government, MEXT KAKENHI (23K08972). MU was supported by a grant from Japanese government, MEXT KAKENHI (24K12706).

Declarations

Competing interests

MH was founding scientist of Otolink Inc. Other authors have no conflicts of interest directly relevant to the content of this article.

Ethical approval

The animal experiments were approved by the Animal Experiment Committee of Keio University (approval number: 11006, 08020) and were performed in accordance with the guidelines of the National Institutes of Health and the Ministry of Education, Culture, Sports, Science, and Technology of Japan.

Additional information

Correspondence and requests for materials should be addressed to M.H.